EPJ Web of Conferences **37**, 09030 (2012)
DOI: 10.1051/epjconf/20123709030

Measurement of $\eta' \to \eta\pi^+\pi^-$ with KLOE and KLOE-2

C.F. Redmer[a] for the KLOE-2 Collaboration

Institute for Physics and Astronomy, Uppsala University, 75120 Uppsala, Sweden
Current address: Institut für Kernphysik, Mainz University, 55128 Mainz, Germany

Abstract. The investigation of $\eta' \to \pi\pi\eta$ allows to study $\pi\pi$ and $\eta\pi$ interactions and the possible influence of the scalar states $f_0(600)$ and $a_0(980)$ on the decay dynamics. 1.7 fb^{-1} of data taken with the KLOE detector at the DAΦNE e^+e^- collider have been analyzed with respect to the charged decay mode $\eta' \to \pi^+\pi^-\eta$. 7900 ± 90 event candidates have been extracted and can be used for a Dalitz plot analysis.

1 Introduction

The hadronic decays $\eta' \to \pi\pi\eta$ are ideal systems to study $\pi\eta$ interactions at low energies. Due to the relatively large center of mass energy and the quantum numbers of the particles in the final state, scalar states like $f_0(600)$ and $a_0(980)$ are favored as intermediate states in $\pi\pi$ and $\pi\eta$ interactions, respectively. In a Dalitz plot the influence of these resonances on the decay dynamics can be studied. However, since the pole masses of both resonances lie outside of the volume of the Dalitz plot and the width of both states is very large, only the effects of the tails of $f_0(600)$ and $a_0(980)$ can be observed.

Different theoretical approaches have been used to describe the decay. Due to the large mass of the η' meson extensions of the chiral perturbation theory (ChPT) have to be applied. Recent approaches include the lowest lying scalar meson candidates into a possible nonet [1], perform calculations in the framework of infrared regularized $U(3)$ ChPT [2], large N_c ChPT, or Resonance Chiral Theory [4], or use a coupled channel Bethe-Salpeter equation as a non-perturbative extension to 1-loop ChPT [3]. The differences of the predicted Dalitz plot densities for different ansatzes and scenarios of contributing resonances are small and call for high precision measurements in order to obtain meaningful results from comparisons of theory and experiment.

The KLOE experiment, located at the DAΦNE e^+e^--collider in Frascati, Italy, has collected an integrated luminosity of 2.1 fb^{-1} at the ϕ meson peak ($\sqrt{s} \simeq 1.02$ GeV/c^2), which corresponds to 7×10^9 produced ϕ and 4×10^5 produced η' mesons, respectively. The KLOE detector is a 4π detector setup, which is able to measure charged as well as neutral particles. It consists of a large volume drift chamber, which provides excellent momentum and vertex reconstruction for charged particles, and a barrel shaped electromagnetic calorimeter, made from lead and scintillating fibers, which surrounds the drift chamber. The energy deposits of charged and neutral particles in the calorimeter are measured with very good energy and time resolution, which allows for the identification of charged particles based on their time of flight. Drift chamber and calorimeter are enclosed in a superconducting solenoid, which is operated at 0.52 T.

The aim of the analysis presented here is a high precision study of the decay dynamics of the charged hadronic decay $\eta' \to \pi^+\pi^-\eta$ based on the data taken at the KLOE experiment.

[a] e-mail: redmer@kph.uni-mainz.de

2 Analysis

1.7 fb^{-1} of the KLOE data have been analyzed with respect to $\eta' \to \pi\pi\eta$ and the subsequent decay $\eta \to \gamma\gamma$. The η' mesons stem from the radiative decay of the ϕ mesons produced in the DAΦNE collider. Thus, events with exactly three photon candidates and exactly two pion candidates have been selected. Photon candidates are identified with clusters in the calorimeter, which are not associated with tracks in the drift chamber. Additionally, the clusters have to fulfill the time constraint $|r_{cl} - ct_{cl}| \sim 0$, must have at least an energy of 10 MeV, and are required to have opening angles relative to other photons of $\sphericalangle(\gamma_i\gamma_j) \leq 18°$. The latter condition is applied to reduce contributions from cluster splitting. A χ^2 test is used to assign the photons candidates to the two-photon decay of the η and the radiative decay of ϕ meson, respectively. As pion candidates two charged tracks are selected, which have opposite curvatures and emerge from a common vertex. The vertex must reside within a cylindrical region of $r \leq 4$ cm and $|z| \leq 8$ cm around the interaction point.

The events selected by these criteria are dominated by the processes $\phi \to \pi^+\pi^-\pi^0$ and $\phi \to \eta\gamma$ with the subsequent decay $\eta \to \pi^+\pi^-\pi^0$, which have a similar topology of the final state and larger cross sections compared to the signal channel.

In order to suppress the background and to improve the accuracy of the measured observables a kinematic fit is performed. Every event is fitted to the hypothesis $\phi \to \pi^+\pi^-\gamma\gamma\gamma$, using momentum and energy conservation as the only constraints. Events with $P(\chi^2_{kf}, ndf) < 0.05$ are rejected.

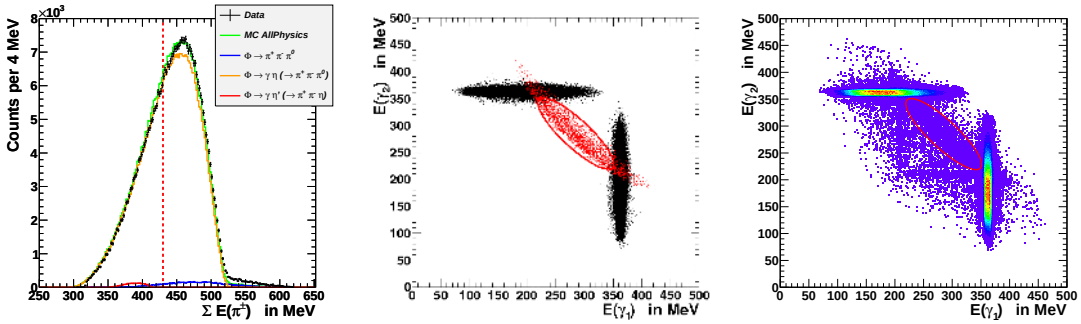

Fig. 1. left: Energy sum of π^+ and π^-. Data (black) are shown along with a complete Monte Carlo simulation (green) and the individual contributions of the decays $\phi \to \pi^+\pi^-\pi^0$ (blue), $\phi \to \gamma\eta(\to \pi^+\pi^-\pi^0)$ (orange), and $\phi \to \gamma\eta'(\to \pi^+\pi^-\eta)$ (red). The dashed line indicates the cut at 430 MeV. **center:** Monte Carlo simulation of the energy correlation of the photons assigned to the $\eta \to \gamma\gamma$ decay for signal $\phi \to \gamma\eta'(\to \pi^+\pi^-\eta)$ (red) and background $\phi \to \gamma\eta(\to \pi^+\pi^-\pi^0)$ (black). **right:** Photon energy correlation from data. The red ellipse illustrates the applied condition.

Further reduction of the background is achieved by a condition on the maximum allowed energy of the charged pions. In the left panel of Fig. 1 the spectrum of the summed pion energies is shown for the events passing the kinematic fit. Data are compared to a complete Monte Carlo simulation (green). Additionally, the individual contributions of the signal decay $\eta' \to \eta\pi^+\pi^-$ (red) and the background from the $\phi \to \pi^+\pi^-\pi^0$ (blue) and the $\eta \to \pi^+\pi^-\pi^0$ (orange) decays illustrated. Events with a summed pion energy larger than 430 MeV are rejected, as indicated by the vertical, dashed line. More than 50% of the background is removed, while the reconstruction efficiency for the signal decay remains unchanged, since the reconstructed maximum pion energy sum is approximately at 415 MeV.

As seen in the left panel of Fig. 1, the data are still dominated by $\phi \to \gamma\eta(\to \pi^+\pi^-\pi^0)$ events. The mono-energetic photon from the radiative decay of the ϕ meson in combination with a soft photon from the π^0 decay fulfills su ficiently well the initial χ^2 test for the photon assignment, as well as the energy and momentum constraints of the kinematic fit. The central panel of Fig. 1 shows the energy correlation of the photons assigned to the $\eta \to \gamma\gamma$ decay from a Monte Carlo simulation of the signal decay and the background from $\eta \to \pi^+\pi^-\pi^0$. While the signal events show a clear anti-correlation of the photon energies, the background is located parallel to the axes due to the constant energy of

360 MeV of the radiative photon from the $\phi \to \gamma\eta$ decay. Thus, the signal can be easily selected with a graphical cut as shown in the right panel of Fig. 1.

For the outlined analysis scheme an efficiency of 17% has been determined in the analysis of Monte Carlo simulations of the signal channel. Fig. 2 shows the resulting invariant mass spectrum of the $\pi^+\pi^-\gamma\gamma$ system obtained from 1.7 fb^{-1} of data. A narrow peak located at the mass of the η' can be observed on top of a continuous background. The background contamination of the peak region is at the level of 11%. The comparison with Monte Carlo distributions shows that $\phi \to \pi^+\pi^-\pi^0$ (orange) and $\phi \to \gamma\eta\,(\to \pi^+\pi^-\pi^0)$ (green) contribute equally to the background. 7900 ± 90 events of the $\eta' \to \pi^+\pi^-\eta$ decay (red) have been reconstructed, which can be used to study Dalitz plot distributions.

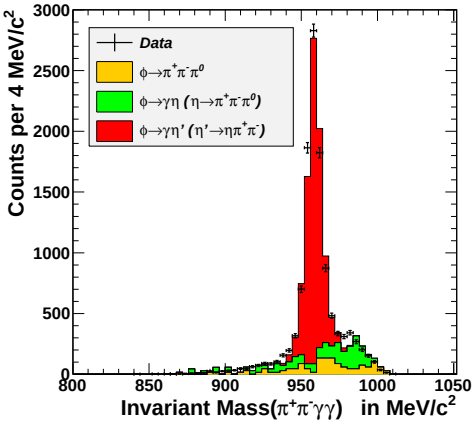

Fig. 2. Invariant mass spectrum of the reconstructed $\pi^+\pi^-\gamma\gamma$ system. The data are show along with MC distributions of the signal $\phi \to \gamma\eta'\,(\to \pi\pi\eta\,(\to \gamma\gamma))$ (red) as well as the background contributions from $\phi \to \pi^+\pi^-\pi^0$ (orange) and $\phi \to \gamma\eta\,(\to \pi^+\pi^-\pi^0)$ (green).

3 Outlook

The statistical accuracy of the discussed analysis is competitive with most of the previous measurements [5]. Further tuning of the individual conditions will allow to increase the extracted number of events. However, the statistics of the recent BES-3 measurement [6] cannot be reached based on the 1.7 fb^{-1} of data taken by KLOE.

A competitive high statistics measurement of $\eta' \to \pi^+\pi^-\eta$ is part of the KLOE-2 project [7]. An upgrade of the DAΦNE collider allows for up to three times higher luminosities compared to the best performance during the KLOE data taking campaigns, so that 5 fb^{-1} could be collected per year. Additionally, the KLOE detector has been enhanced by new subdetectors. An inner tracker made of four layers of cylindrical triple GEMs will improve the vertex resolution and increase the efficiency for low momentum particles, new calorimeters at small scattering angles will increase the acceptance for photons and taggers for leptons scattered at small angles will allow to perform tagged measurements of hadron production in $\gamma\gamma$ collisions.

References

1. A. Fariborz and J. Schechter, Phys. Rev. **D60**, (1999) 034002
2. N. Beisert and B. Borasoy, Nucl. Phys. **A716**, (2003) 186
3. B. Borasoy and R. Nissler, Eur. Phys. J **A26**, (2005) 383
4. R. Escribano, P. Masjuan and J. J. Sanz-Cillero, JHEP **05**, (2011) 094
5. G. R. Kalbfleisch, Phys. Rev. **D10**, (1974) 916
   CLEO Collaboration (R. A. Briere *et al.*), Phys. Rev. Lett. **84**, (2000) 26
   V. Dorofeev *et al.*, Phys. Lett. **B651**, (2007) 22
6. BES-III Collaboration, Phys. Rev. **D83**, (2011) 012003
7. KLOE-2 Collaboration (G. Amelino-Camelia *et al.*), Eur. Phys. J. **C68**, (2010) 619